

We are IntechOpen, the world's leading publisher of Open Access books Built by scientists, for scientists

5,000

Open access books available

125,000

International authors and editors

140M

Downloads

Our authors are among the

154

Countries delivered to

TOP 1%

most cited scientists

12.2%

Contributors from top 500 universities



WEB OF SCIENCE™

Selection of our books indexed in the Book Citation Index
in Web of Science™ Core Collection (BKCI)

Interested in publishing with us?
Contact book.department@intechopen.com

Numbers displayed above are based on latest data collected.
For more information visit www.intechopen.com



Chapter

Influence of the Wavelength of Excitation and Fluorescence Emission Detection on the Estimation of Fluorescence-Based Physiological Parameters in Different Classes of Photosynthetic Organisms

*Stefano Santabarbara, William Remelli,
Anastasia A. Petrova and Anna Paola Casazza*

Abstract

Fluorescence-based methodologies are commonly employed to determine a wide spectrum of physiological parameters in intact photosynthetic organisms. These methods rely on the detection of Chlorophyll a fluorescent emission, which exhibits changes in its intensity due to the occurrence of quenching phenomena of either photochemical or non-photochemical nature, as well as in response of the absorption cross-section of the photosystems. At room temperature, it is generally considered that most of the emission stems from Photosystem II, and therefore, most of the physiological parameters rely on the assumption that contribution from Photosystem I is negligible. Moreover, it is often considered that the whole light-harvesting antenna is efficiently coupled to either of the photosystems and does not contribute, independently, to the detected emission. When these caveats are not realised, fluorescence-based indicators might be subjected to biases that tend to underestimate the extent of both photochemical and non-photochemical quenching. The contribution of Photosystem I and partially coupled/antenna components can be assessed through the analysis of the dependency of steady-state emission as a function of both the excitation and the emission wavelengths. On this basis, methods relying on using different combinations of excitation and emission wavelengths will be discussed in order to minimise the bias on the estimation of physiologically relevant parameters.

Keywords: chlorophyll fluorescence, maximal photochemical efficiency, photochemical quenching, non-photochemical quenching, Photosystem II, Photosystem I, light harvesting complexes, phycobilisomes

1. Introduction

Methodologies relying on the monitoring of Chlorophyll (Chl) *a* fluorescence emission have a very widespread application in photosynthesis research and have therefore been amply adopted by the scientific community (for a comprehensive survey, see the quite recent monography edited by [1]). Since Chls are fundamental pigments, naturally coordinated by the photosynthetic photosystems, these fluorescence-based methods do not require the use of exogenous dyes, or their coordination to specific biological targets. Thus, techniques based on Chl-fluorescence monitoring have become popular as they allow to address a spectrum of physiologically related questions, non-invasively, with relatively fast temporal responses and high sensitivity. Moreover, these methods are suitable for both *in vitro*, i.e. on isolated photosynthetic membranes or Chl-protein complexes, and *in vivo*, either on leaves or unicellular and multicellular algae. Furthermore, they can be used in combination with other analytical approaches, such as gas exchange and/or transmission/reflectance changes, without extensive cross-interference. Noteworthy, fluorescence detection strategies are often the method of choice for remote sensing as well, especially when, although not exclusively, sunlight can be used as the excitation source.

The most widely employed physiological measurements based on chlorophyll fluorescence detection are the determination of fluorescence quenching processes resulting either from photochemical reactions (photochemical quenching), or regulatory processes affecting the fluorescence emission yield, collectively referred to as non-photochemical quenching (NPQ).

1.1 Photochemical quenching

Photochemical quenching is the process through which the emission yield of protein-bound Chl is decreased in response to energy conversion reactions occurring in photochemically active pigments, the reaction centre (RC), of a photosystem. Historically, the occurrence of fluorescence quenching as a response to the redox state of the terminal electron acceptors, Q_A and Q_B (e.g. [2–4]) of PSII, and similarly in the reaction centre of purple bacteria which shares some functional similarities, paved the way for the now amply diffused utilisation of fluorescence measurements to determine physiological parameters. The fluorescence yield of PSII is low when the electron acceptors are oxidised (F_0 , open centres) and reaches a maximal value when the redox centre Q_A is reduced (F_M , closed centres). The difference between the maximal fluorescence level and the minimal one is defined as variable fluorescence ($F_V = F_M - F_0$).

The maximal fluorescence level can be promoted either by brief, intense, light pulses, or flashes that cause the almost complete reduction of PSII acceptor pool (saturating pulses or flashes), so that Q_A is reduced as well, or using inhibitors, like 3-(3,4-dichlorophenyl)-1,1-dimethylurea (DCMU), that inhibit the oxidation of reduced Q_A^- by Q_B (e.g. [1, 3–5]). When inhibitors are used, the F_M condition is attained even when employing low actinic illumination, such as the measuring beam in a conventional fluorescence measurement, so that the use of additional saturating pulses could be avoided.

The conclusive demonstration that the differences in the emission intensity under F_0 and F_M conditions correspond to an effective change in fluorescence yield came from fluorescence lifetimes investigation, where it was shown that under open centre conditions the average fluorescence lifetimes, for the whole PSII supercomplex composed of its core complex and external antenna complement is in the order of 200–300 ps, whereas upon centre closures, it reaches values of

1.2–1.5 ns (e.g. [6–10]), that is, the same 3- to 5-fold increase observed by steady-state/pre-steady-state methods.

It can then be straightforwardly demonstrated, and it is therefore commonly accepted, that the maximal photochemical quantum efficiency of PSII, $\Phi_{PC,PSII}^{\max}$, could be estimated with sufficiently good approximation by the ratio of the variable and maximal fluorescence levels, i.e. by F_V/F_M (e.g. [1, 3–5]). The relation follows from considering that F_0 and F_M level could be described by the following expressions:

$$\left\{ \begin{array}{l} F_0 = \alpha\phi_0 = \alpha \frac{k_f}{\sum_i k_i + K_{pc}\gamma_{Q,0}} \\ F_M = \alpha\phi_M = \alpha \frac{k_f}{\sum_i k_i + K_{pc}\gamma_{Q,M}} \end{array} \right. \quad (1)$$

where α is a factor depending on the number of photons absorbed at the excitation wavelength and emitted at the detection wavelength, which is independent of the redox state of the acceptors in the RC, ϕ_0 and ϕ_M are the fluorescence emission yield at open and closed centres, respectively, which could be further expressed in terms of probabilities of the excited state de-excitation by fluorescence (k_f), with respect to the sum of all the so-called natural de-excitation processes, including fluorescence, $\sum_i k_i$ and quenching by photochemistry, here described in terms of a macroscopic, rather than molecular rate constant, K_{pc} , weighted by the molar fraction of oxidised electron acceptors at open ($\gamma_{Q,0}$) and closed centres ($\gamma_{Q,M}$). Considering that $\gamma_{Q,0} = 1$ and $\gamma_{Q,M} = 0$, that is, in the case of PSII, Q_A being completely oxidised and reduced, and substituting into Eq. (1), results in:

$$\frac{F_V}{F_M} = \frac{K_{pc}}{\sum_i k_i + K_{pc}} \approx \Phi_{PC,PSII}^{\max} \quad (2)$$

Although the above-presented derivation presents the yield in the form of the so-called “lake model”, in which the quenching induced by photochemistry is shared over a large pool of photosystems, thereby approaching the classic Stern-Volmer description, for the F_0 and F_M level, identical conclusion would be reached by considering either separate units or partial connectivity, under the condition that *all* centres are either open or closed. On the other hand, these models do differ significantly in the description of any intermediate level between F_0 and F_M , that is, for as any value of γ_Q different from 0 or 1, which manifests either in the kinetics or rise to F_M (so-called induction curve) or in the steady-state levels, F_{ss} , determined by a given background illumination. It is also worth noticing that Eq. (2) is valid, provided that the *only* quenching process differing at F_0 and F_M is strictly due to a modulation of photochemical quenching. It is however being shown that the fluorescence level reached by single-turnover flashes can be slightly lower than those observed under the so-called multiple turnover pulses, or by continuous illumination, indicating that the estimation of $\Phi_{PC,PSII}^{\max}$ from F_V/F_M could be somewhat biased (e.g. [11, 12]). However, in general, these processes, whose molecular nature remains to be fully determined, lead to contained distortions in photochemical yield estimation. Therefore, since measurements of F_V/F_M are relatively rapid, they remain one of the most employed indicators to determine not only PSII quantum yield, but also its changes in response to stress, both in the laboratory and in the field. Measurements of variable fluorescence in the presence of actinic backgrounds

also have become a widespread practise to gain information concerning photosynthetic electron transport. A number of indicators have been proposed in order to extract this information from fluorescence data and, at least for land plants, strong correlation with simultaneous gas-exchange measurements has been demonstrated [5, 13, 14]. This is because the variation in the amplitude of F_V in the presence of actinic illumination, in combination with changes in the F_M level, with respect to the dark-adapted state, could be related to the fraction of “open/closed” PSII centres as well as to their photochemical quantum yield under operation conditions. A detailed discussion of the parameters is beyond the scope of this chapter, but several approaches are reported in the recent monography [1] and extended review [5] on these topics. We limit to notice that the interpretation of F_V -related fluorescence indicators in the presence of an actinic illumination is less straightforward than for dark adapted conditions.

1.2 Non-photochemical quenching

On top of photochemical quenching processes, fluorescence monitoring finds its natural application in the study of regulative mechanisms of light harvesting efficiency, which manifest themselves principally as a quenching of the Chl fluorescence emission. The establishment of non-photochemical quenching (NPQ) results in the lowering of the F_M level in response to actinic illumination regimes close to or exceeding the saturation of the photosynthetic electron transport capacity (e.g., [15, 16]). The fluorescence level in the presence of a non-photochemical quenching, most commonly measured at closed centres by the application of multiple turn-over saturating pulse, is referred to as F'_M and can be described, similarly to F_M , within a lake model approximation as follows:

$$F'_M = \alpha \frac{k_f}{\sum_i k_i + [Q_{NP}] \cdot K_{Q, NP}} \quad (3)$$

where $K_{Q, NP}$ and Q_{NP} are the macroscopic quencher rate constant and the concentration of the non-photochemical quencher, respectively. These two quantities are however difficult to assess separately and are generally determined as the product $[Q_{NP}] \cdot K_{Q, NP}$ through the NPQ parameters (note in the following the italics will identify the parameters whereas upright capitals indicate the process), that is defined as $F_M/F'_M - 1$, with the definitions in Eqs. (1) and (3) as follows:

$$NPQ = \frac{F_M - F'_M}{F'_M} = [Q_{NP}] \cdot \frac{K_{Q, NP}}{\sum_i k_i} \quad (4)$$

NPQ has proven to be a very complex phenomenon, showing several phases of development, upon light exposure, and relaxation, upon return to darkness [15, 16], that despite the generality of its manifestation, depends strongly on the organism or at least the class of organisms in which it is investigated [17, 18]. This large variability is likely due to the generally accepted knowledge that NPQ processes occur principally, when not exclusively, in the external antenna complement of PSII [15–18]. Whereas the core complex, which serves as an internal light harvesting system as well as the photochemical reaction centre, is well conserved amongst different oxygenic photosynthetic organisms [19], the composition of the external antenna is instead very diversified, having evolved to optimise light harvesting in ecological niches possessing different spectral distributions either in terms of light

spectrum or light intensity [20, 21]. Hence, it is not surprising that also adaptive responses to changes in light conditions vary significantly in different organisms.

1.3 Source of possible distortion due to emission from Photosystem I and decoupled light-harvesting antenna

One of the caveats behind Chl-based fluorescence indicators is the assumption that the monitored fluorescence is emitted exclusively or almost exclusively from PSII. This is, in general, a justified assumption since, particularly under closed centres conditions, and at a room temperature or temperatures covering the “physiological interval” of living organisms, the fluorescence yield of PSII could be several folds larger than the one of the other ubiquitous component of the electron transfer chain, Photosystem I (PSI). Measurements on PSI isolated from different species indicate that its average fluorescence lifetime is in the order of 20–40 ps [19, 22, 23], that is, 5–10 times faster than for the PSII-antenna supercomplex at open centres and 200–500 faster at closed centres, in the absence of non-photochemical quenching [6–11]. Similar results concerning PSI lifetimes are also retrieved for measurements when the photosystem is embedded in the thylakoid membranes [8, 9, 24]. Moreover, PSI does not show a significant change in emission yield upon oxidisation of the terminal donor, P_{700} [25]. Hence, differently from PSII, PSI does not exhibit any significant induction, so that, in practise, its contribution to the cell emission is expected to be larger under F_0 than F_M conditions. Direct comparison of lifetimes and steady state emission levels holds, however, provided that the photosystems are in close stoichiometric ratio, that they absorb almost the same number of photons at the excitation wavelength and also have the same emission bandwidth at the excitation wavelength. For instance, in most cases, PSI emission results red-shifted with respect to that of PSII (e.g. [19, 22, 23] and references therein), so that its contribution to the detected fluorescence emission from photosynthetic material is expected to be a function of the detection wavelength, which depends on the specific emission spectra of PSII and PSI in a given organism. Similarly, either the absorption or the relative stoichiometry, hence the fraction of excitation photons absorbed by each photosystem, are expected to be dependent on organism. Especially for the determination of F_0 , contribution from PSI emission could become significant and not necessarily negligible [24, 26–28], and similarly for cases in which the F'_M level is quenched significantly below F_M .

Another possible source of distortion in the determination of these fluorescence levels is the contribution from populations of the external antenna not coupled in terms of energy transfer to the core of either PSII or PSI. Differently from PSI, the core-decoupled pigment-protein complexes of the antenna are very bright in terms of fluorescence, emitting with lifetimes comparable or longer than PSII at closed centres. Typically, the population of decoupled antenna tends to be vanishingly small in most organisms having transmembrane light-harvesting apparatus [27, 29], but it can be sizable in cyanobacteria, accounting for 1–5% of the external antenna [26, 30, 31] and therefore clearly contributing to the cellular emission [26–28, 32–34]. Thus, differences between organisms, which harbour diversified external antenna complements, are to be expected.

2. Spectral dependence of the F_V/F_M ratio

A strategy to verify the distortion originating from the emission due to either PSI or a fraction of decoupled/weakly coupled external antenna components to the

determination of the F_V/F_M ratio is that of recording the steady-state fluorescence emission spectrum of photosynthetic material under open PSII RC conditions, by using a low-intensity excitation having minimal actinic effect thereby approaching the real dark-adapted F_0 level, hereafter these will be referred to as F'_0 , and to compare it with the spectrum obtained for the same excitation regime in the presence of an inhibitor, such as DCMU, that promotes PSII centres closure, thereby reaching the F_M conditions. The expectation is that when the fluorescence spectra are effectively dominated by PSII emission, the F_V/F_M ratio (or analogously the F_M/F_0 ratio) will attain the same value, irrespectively on the detection wavelength. Similarly, recording the emission spectra under F'_0 and F_M conditions, but at different excitation wavelengths, the expected result in the absence of distortion is that the F_V/F_M ratio is not only independent of the observation wavelength but also from the one of excitation. Contributions from either PSII or decoupled antenna, or both, would result in an observation-wavelength dependency of the F_V/F_M value, which might also depend on the excitation [26–28, 32–36].

In the successive paragraphs, experiments performed in model green algae (*Chlorella sorokiniana* and *Chlamydomonas reinhardtii*) and model cyanobacteria (*Synechocystis sp.* PCC6803 and *Synechococcus sp.* PCC7942) are summarised, because these classes of organisms display significant differences [27].

Conceptually, these types of experiments are pretty simple, but technically they might be challenging as they require a rather sensitive apparatus in order to collect F'_0 spectra with sufficient signal-to-noise ratio, due to the low intensity of the excitation beam. On the other hand, recording the emission under F_M conditions is relatively straightforward and will therefore be suggested as an initial screening for possible sources of bias in the F_V/F_M , and thus $\Phi_{PC,PSII}^{Max}$, estimations.

2.1 Excitation and emission dependency in model green algae

The emission spectra recorded under F'_0 and F_M conditions in the green algae *C. sorokiniana* and *C. reinhardtii* for excitation at 435, 475, 520 and 570 nm are shown in **Figure 1**. These wavelengths were chosen as they represent preferential excitation of Chl *a* (435 nm) and Chl *b* (475 nm), which are the main pigments in green algae, where Chl *a* is present both in the core complexes and the external antenna, and Chl *b* is present only in the light-harvesting complexes associated with both PSII and PSI. Although the external antenna complement is composed by several Chl-protein complexes, it is convenient in this case in which the individual contributions cannot be discriminated, to refer to them collectively as LHCI and LHCII, for PSI and PSII, respectively. Excitations at 520 and 570 nm are relatively unselective in this class of organisms, but they represent preferential excitation for phycobilisomes (PBS), which represent the main, often the only, external antenna complement in cyanobacteria.

For ease of comparison, the spectra, at each excitation wavelength, are normalised to the maximum of the F_M spectrum, and the F'_0 one is scaled accordingly. The spectra reported in **Figure 1** demonstrate that in both model green algae, the emission bandwidth displays a very weak dependency on the excitation wavelength, and that, as better appreciable in the insets where each spectrum is normalised to its maximum, the overall bandwidth shows only limited differences between F'_0 and F_M conditions. Yet, the spectra recorded at F'_0 show a slight increase in the relative intensity in the 700–730 nm window, with respect to those recorded at F_M . This difference can be interpreted, dominantly, by a relatively

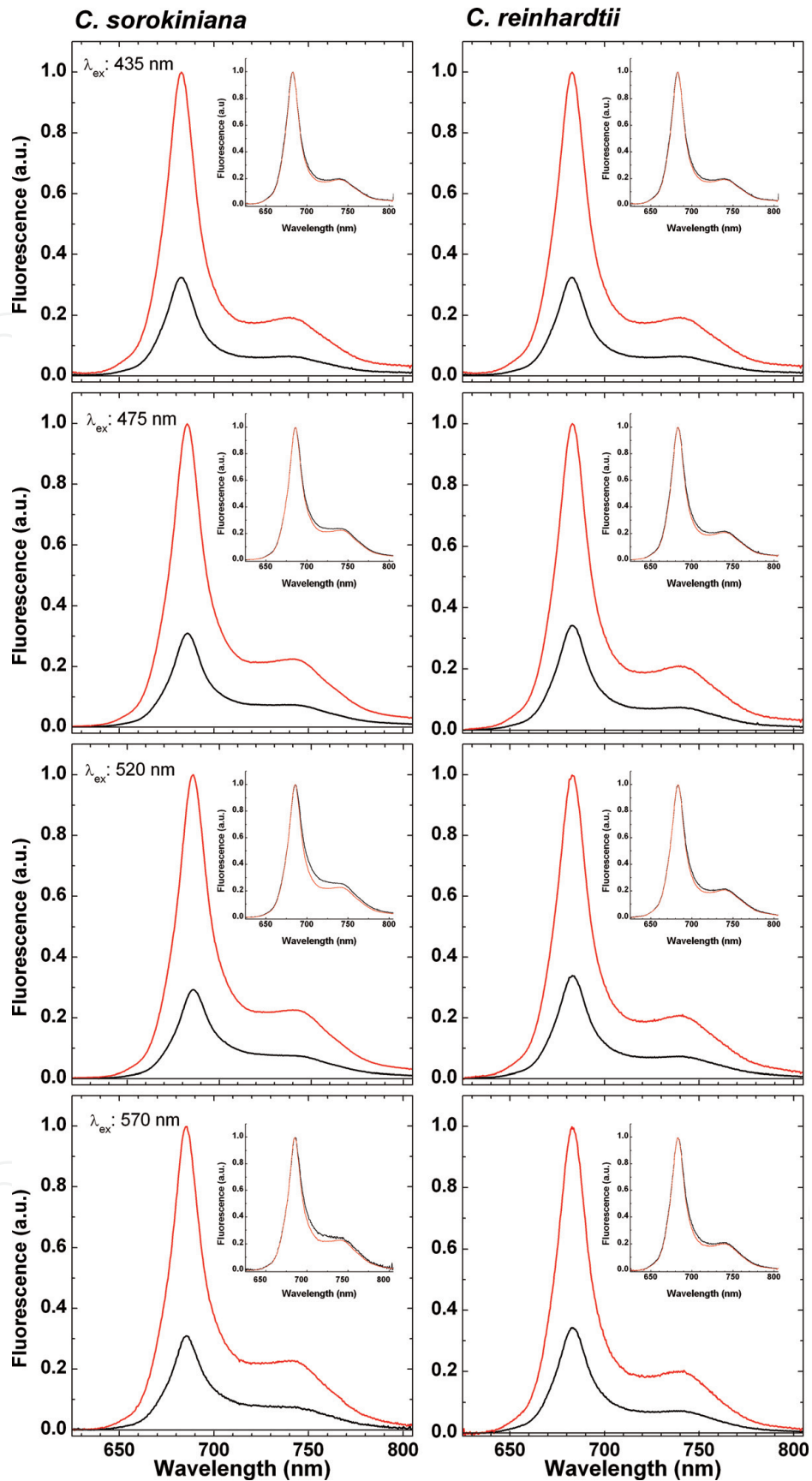


Figure 1. Emission spectra recorded under F_0 (black lines) and F_M (red lines) conditions in the model green algae *C. sorokiniana* (left) and *C. reinhardtii* (right), at room temperature, for excitation at 435, 475, 520 and 570 nm. The spectra in the main panels are normalised and scaled to the maximal emission at F_M . The insets show the spectra normalised each at its maximal emission. The samples were diluted to an optical density (scatter compensated) in between 0.05 and 0.1 OD at the maximal absorption in the red, at 680 nm. The excitation bandwidth was between 0.5 and 1 nm (FWHM); spectra were acquired with a resolution of 0.25 nm and are corrected for the sensitivity of the detector. Further details on the experimental set-up are described in Refs. [24, 26,27].

larger contribution of PSI emission in this wavelength region, when PSII fluorescence is quenched photochemically [24, 27].

In **Figure 2** are shown the F_V/F_M spectra, obtained from data of **Figure 1**. For both model green algae, the F_V/F_M spectra are indeed quite flat across the whole emission band, showing however a trough, corresponding to minimal values, in the 700–740 window, in correspondence to the maximal *in vivo* emission of PSI. Maximal values are recorded close to maximal cellular emission, with values ranging in 0.66–0.72 interval, that is dominated by PSII instead, corresponding to an underestimation of F_V/F_M of 5–8% with respect to its maximal value. It is also worth remarking that the F_V/F_M values have a rather limited dependency on the excitation wavelength, which is probably for the results reported here, within the limits of the actinic effect of the excitation beam at F'_0 , determining a condition which more (for larger F_V/F_M) or less (for lower F_V/F_M) closely approaches the actual F_0 .

A strategy to extract the *in vivo* emission spectrum of PSII is that of calculating the F_V spectra, which are shown in **Figure 3**, each normalised to its maximal value. It is clear then that the bandshape of the F_V spectra does not depend on the excitation wavelength. This is a key indication, supported by parallel fluorescence lifetime evidences [24], that the observed spectral dependence of the F_V/F_M spectrum is not due to, and certainly not dominated by, an intrinsic spectral dependency of photochemical quenching in PSII.

Figure 3 also shows a comparison for the normalised F_M spectra, highlighting their very limited dependency on the excitation wavelength. As mentioned above, the recording of spectra at F_M is attained more straightforwardly than that at F'_0 , as it does not suffer from possible biases from the actinic effect of the excitation wavelength. Although the spectra shown here were acquired using the same excitation intensity at F'_0 and F_M , in general, the latter can be collected with higher excitation fluxes henceforth in conventional instruments. Care shall however be taken to avoid the onset of non-photochemical quenching processes. The invariance of the emission bandshape of the F_M spectrum with respect to the excitation wavelength can be considered as a preliminary verification that this experimental condition does not affect the measured F_V/F_M ratio.

To better compare the effect of excitation and detection wavelengths in determining the F_V/F_M ratio in traditional set-ups where detection is commonly performed using interferential or band-pass filters, F'_0 and F_V/F_M were calculated convolving the emission spectra with either ideal interferential (FWHM 10 nm) or band-pass filters. The results obtained are listed in **Table 1**, all normalised to F_M . Maximal values of F_V/F_M (corresponding to minimal ones of F'_0) are obtained for detection centred at ~685 nm and minimal at 715 nm, for the conditions tested here. Similarly band-pass with cut-on filter having a threshold frequency above 700 nm yielded lower F_V/F_M values than for shorter-wavelengths, which integrate over a larger portion of the emission band.

2.2 Excitation and emission dependency in model cyanobacteria

The emission spectra recorded under F'_0 and F_M conditions in two model cyanobacteria, *Synechocystis sp.* PCC 6803 and *Synechococcus sp.* PCC7942 (from now on referred simply as *Synechocystis* and *Synechococcus*), and at different excitation wavelengths are shown in **Figure 4**. Differently from what reported in **Figure 1** for model green algae, in both model cyanobacteria, the emission bandshapes display a strong dependency both on the excitation wavelength and on the redox conditions

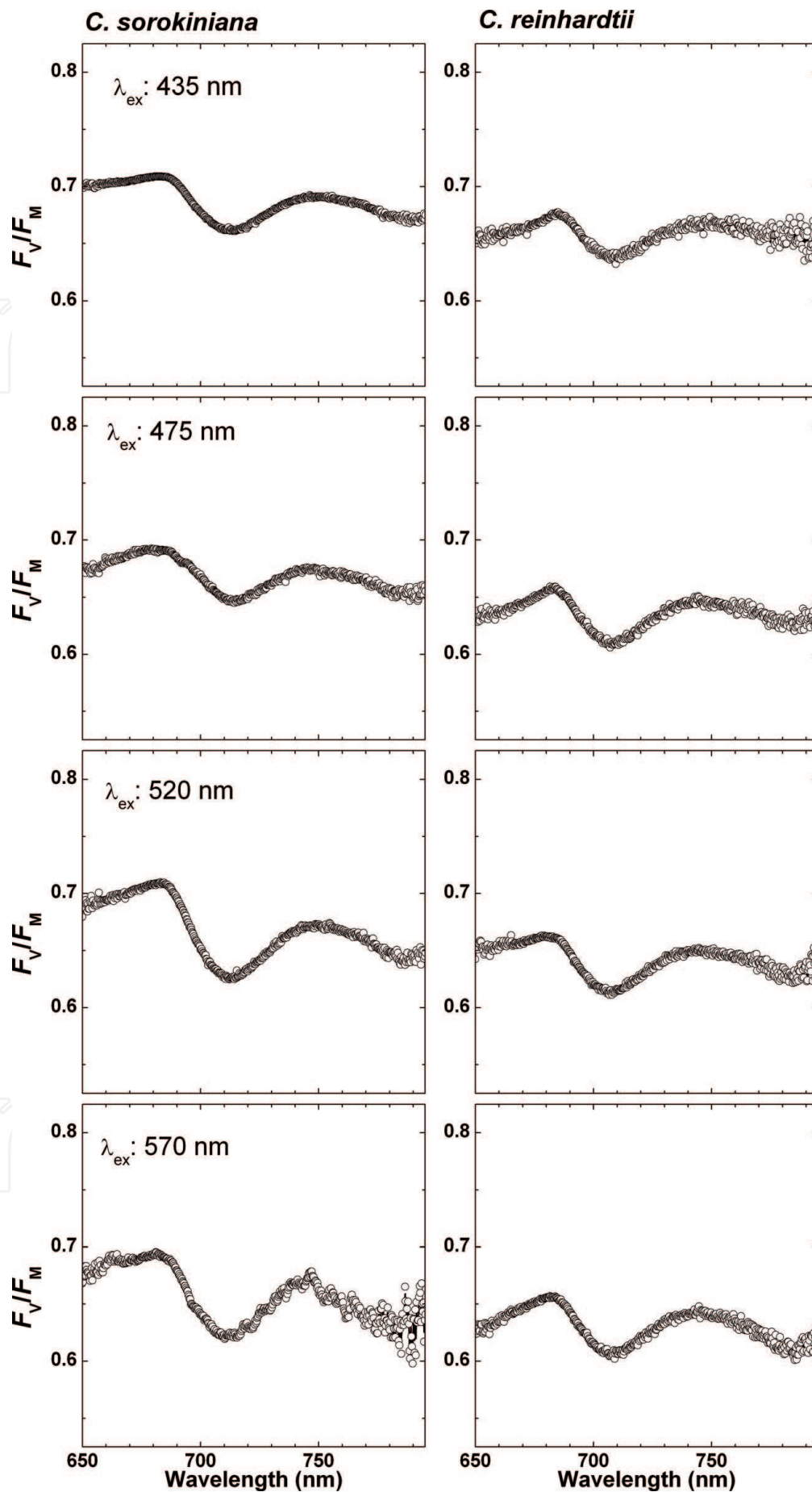


Figure 2. Emission wavelength dependency of the F_V/F_M ratio in *C. sorokiniana* (left) and *C. reinhardtii* (right), at room temperature, for excitation at 435, 475, 520 and 570 nm, calculated from the spectra of **Figure 1**.

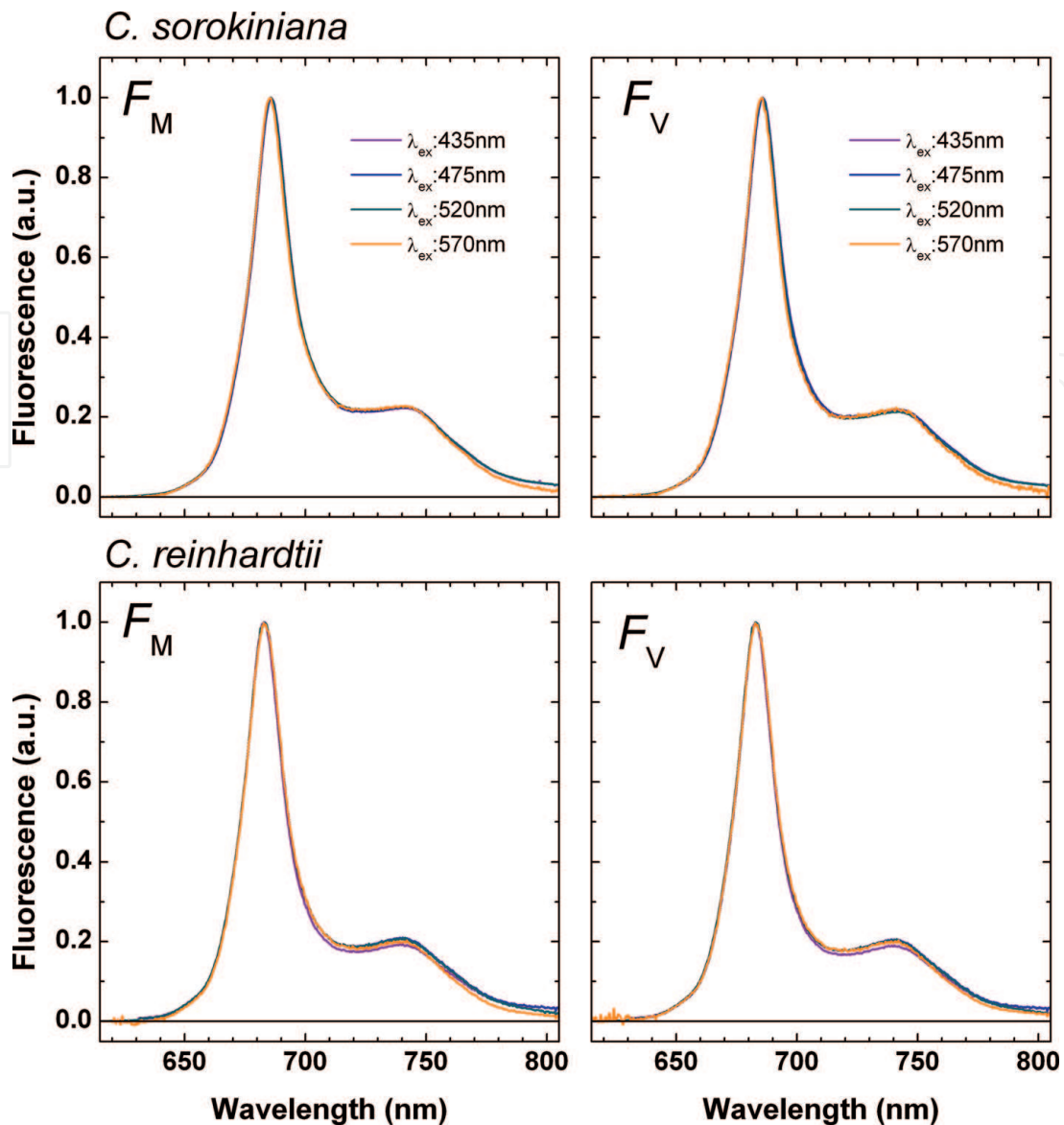


Figure 3.

Comparison of the normalised F_M and calculated $F_V = F_M - F'_0$ emission spectra, in *C. sorokiniana* (top) and *C. reinhardtii* (bottom), at room temperature, for excitation at 435 nm (violet), 475 nm (blue), 520 nm (green) and 570 nm (orange). Each spectrum is normalised to its maximum value.

of the PSII acceptors. Upon excitation at 435 and 475 nm, the main peak is centred at 684 nm and intense shoulders, more pronounced than what is observed in green algae, are observed on the long wavelength range above ~ 700 nm. Moreover, a relatively intense blue wing is clearly observed in the 610–660 nm range, which becomes larger and even dominant when the sample is excited at 520 and 570 nm, that is, for preferential excitation in the PBS antenna, where a clear satellite peak centred at 600 nm is discernible. It is immediately noticeable that the short wavelength emission displays negligible variation in intensity when PSII centres are closed with respect to when they are open.

This is further highlighted in **Figure 5**, where the F_V/F_M spectra derived from the data of **Figure 4** are reported. The results show that although the details depended on the species, in general, in both model cyanobacteria, the F_V/F_M value displays a significant dependence both on the wavelength of detection as well as on the wavelength of excitation. For excitation at 435 nm, that is preferential for Chl *a* (and carotenoids), maximal F_V/F_M values are obtained, in correspondence to the fluorescence emission peak (675–685 nm), in the 0.6 range. However, even when

<i>C. sorokiniana</i>								
Excitation	435 nm		475 nm		520 nm		570 nm	
Interferential (Centre, nm)	F'_0	F_V/F_M	F'_0	F_V/F_M	F'_0	F_V/F_M	F'_0	F_V/F_M
650	0.302	0.698	0.325	0.675	0.310	0.690	0.319	0.681
670	0.292	0.708	0.312	0.688	0.298	0.702	0.311	0.689
680	0.292	0.708	0.309	0.691	0.293	0.707	0.308	0.692
690	0.304	0.696	0.315	0.685	0.305	0.695	0.319	0.681
700	0.327	0.673	0.330	0.670	0.342	0.658	0.353	0.647
720	0.347	0.653	0.349	0.651	0.366	0.634	0.370	0.630
Bandpass (cut-on, nm)								
655	0.314	0.686	0.325	0.675	0.323	0.677	0.334	0.666
675	0.317	0.683	0.326	0.674	0.326	0.674	0.336	0.664
695	0.331	0.669	0.336	0.664	0.347	0.653	0.354	0.646
720	0.327	0.673	0.335	0.665	0.341	0.659	0.348	0.652
<i>C. reinhardtii</i>								
Inteferential (Centre, nm)	F'_0	F_V/F_M	F'_0	F_V/F_M	F'_0	F_V/F_M	F'_0	F_V/F_M
650	0.343	0.657	0.365	0.635	0.348	0.652	0.371	0.629
670	0.336	0.664	0.354	0.646	0.341	0.659	0.352	0.648
680	0.328	0.672	0.346	0.654	0.339	0.661	0.346	0.654
690	0.330	0.670	0.353	0.647	0.350	0.650	0.355	0.645
700	0.350	0.650	0.377	0.623	0.375	0.625	0.381	0.619
720	0.352	0.648	0.377	0.623	0.372	0.628	0.381	0.619
Bandpass (Cut-on, nm)								
655	0.337	0.663	0.359	0.641	0.353	0.647	0.361	0.639
675	0.337	0.663	0.360	0.640	0.355	0.645	0.362	0.638
695	0.345	0.655	0.369	0.631	0.365	0.635	0.374	0.626
720	0.340	0.660	0.361	0.639	0.357	0.643	0.367	0.633
Values of F'_0 and F_V/F_M determined from the F'_0 and F_M emission spectra of model green algae, after convolution with either ideal interferential filter (Gaussian, FWHM 10 nm) or long-pass filter (cut-on transitions 4 nm at the indicated 50% transmission). Values are normalised to $F_M = 1$ under each excitation/emission condition.								

Table 1. Estimated F'_0 and F_M detected through interferential and band-pass filters in green algae.

monitoring F_V/F_M at the emission maxima, its value depends on the excitation wavelength, decreasing to 0.45–0.5 for all other wavelengths tested. Moreover, in both organisms and for all excitations, the F_V/F_M ratio decreases sharply in the 700–730 nm window, to values of 0.2–0.3, corresponding to ~40% underestimation with respect to the maximal. Similarly to what was discussed for the case of green algae, this decrease can be ascribed to a significant contribution of PSI emission, especially at F'_0 , in this wavelength region [26, 27]. The effect is however much larger than in green algae. This could be explained by differences in antenna properties for these two classes of organisms, as well as in the PSI:PSII stoichiometries. Whereas for excitation in the blue, PSI and PSII absorb almost equal fractions of photons, in cyanobacteria, the difference is larger as each

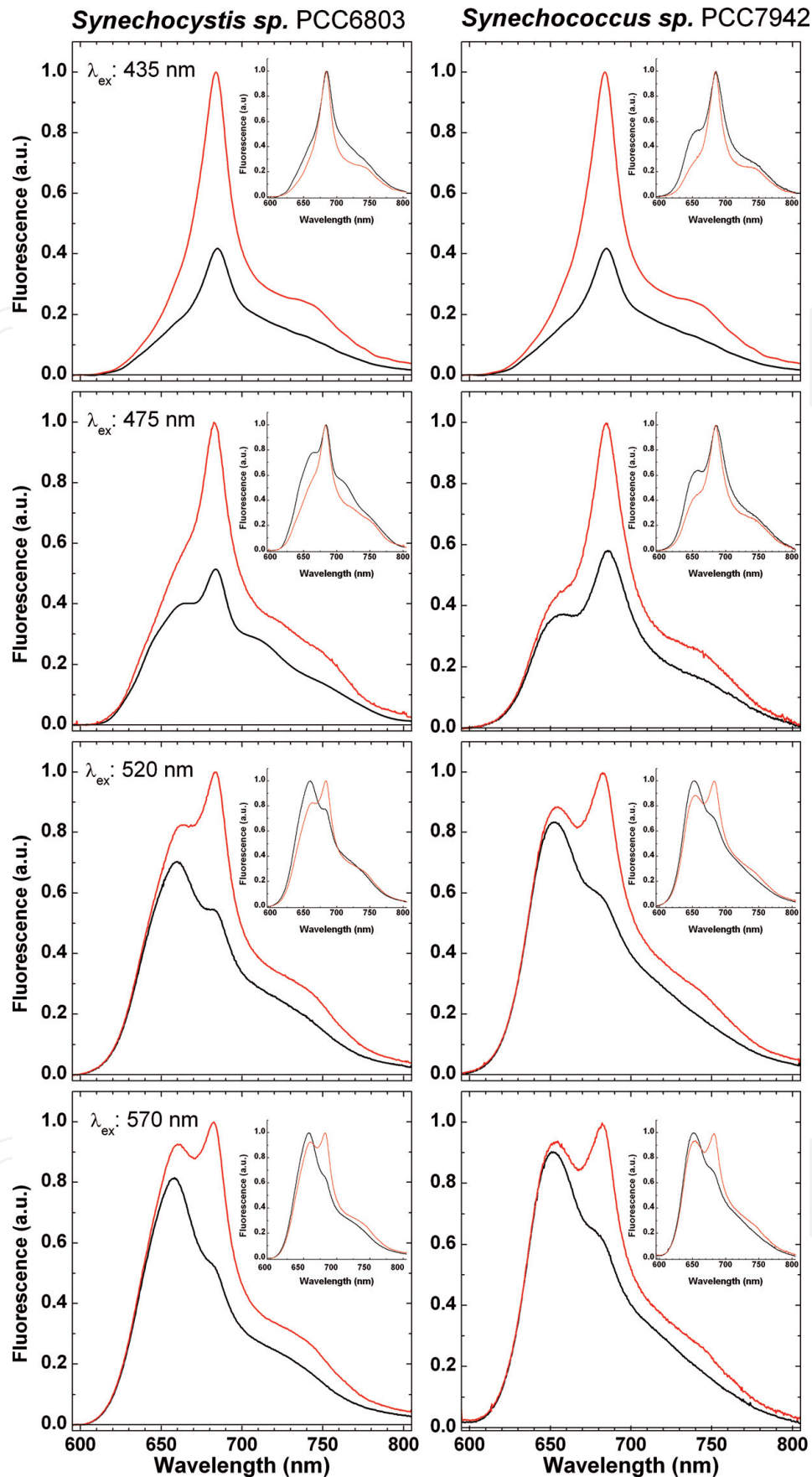


Figure 4. Emission spectra recorded under F'_0 (black lines) and F_M (red lines) conditions in the model cyanobacteria *Synechocystis sp. PCC6803* (left) and *Synechococcus sp. PCC7942* (right), at room temperature, for excitation at 435, 475, 520 and 570 nm. The spectra in the main panels are normalised and scaled to the maximal emission at F_M . The insets show the spectra normalised each at its maximal emission.

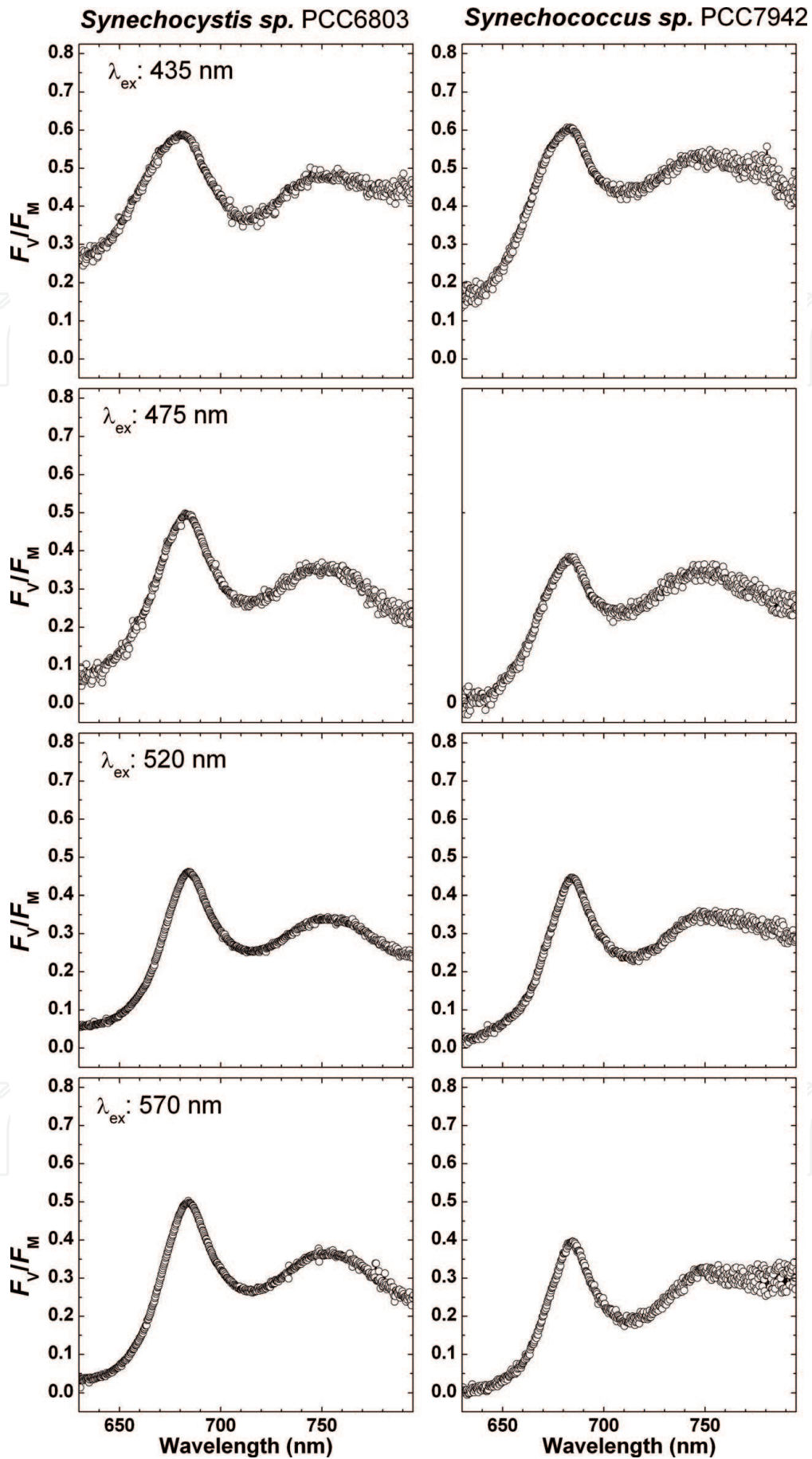


Figure 5. Emission wavelength dependency of the F_V/F_M ratio in *Synechocystis sp. PCC6803* (left) and *Synechococcus sp. PCC7942* (right), at room temperature, for excitation at 435, 475, 520 and 570 nm, calculated from the spectra of **Figure 4**. Please note the difference in the y-scale with respect to **Figure 2**.

monomeric PSII core binds about 45 Chl *a* molecules, whereas PSI monomers bind about 90 Chl *a*. Furthermore, whereas PSII is a functional dimer (total ~ 90 Chls), PSI is, at least as the most abundant form, a trimer (270 Chls). Even for a 1:1 ratio of the two supercomplexes, PSI is expected to absorb about 3 times more photons than PSII. Moreover, it is often reported that the PSI:PSII stoichiometry in cyanobacteria could be much larger than 1, and thereby, PSI will result contributing significantly to the steady state emission despite its low fluorescence quantum yield.

Furthermore, the F_V/F_M spectra in model cyanobacteria display a very steep decrease to a minimal value on the blue emission wing, below ~ 665 nm, in correspondence to PBS emission. The decrease in F_V/F_M is much steeper when the external antenna is excited directly (520 and 570 nm, in **Figure 5**, and reaching negligible values well below 0.1). At least for the case of *Synechocystis*, this applies moreover to all wavelengths at which PBS absorption is dominant [27]. Hence, monitoring F_V/F_M on the short emission wing leads to profound underestimation of the maximal photochemical yield of PSII.

However, the bandshape of the F_V spectra does not depend significantly on the excitation wavelength, as also observed in model green algae. In the case of model cyanobacteria, a more pronounced wing extending down to 625–630 nm is visible (**Figure 6**) in the F_V spectra. This could be ascribed to variable fluorescence of the energetically coupled fraction of the PBS antenna, at least of its terminal emitters [27, 37, 38]. The relative invariance indicates that the changes in the F_V/F_M value are not dominated by an intrinsic variation of photochemical quenching over the PSII emission band (see discussion in ref. [27] for further detail), rather to the overlapped contributions of different chromophore-protein supercomplexes, nominally PSI and a fraction of the PBS antenna which is not energetically coupled to the core complexes of either PSI or PSII. The need for considering an energetically uncoupled antenna stems from the large increase in its emission upon direct excitation and the close-to-absent photochemical quenching, which is to be expected for a core-coupled antenna. It is also demonstrated by the long fluorescence lifetimes (1–4 ns, cite), even under open PSII RC conditions.

In **Figure 6** are also shown the normalised F_M spectra recorded at different excitation wavelengths. It is immediately noticeable that the bandshape of the F_M spectra, differently from the case of green algae and the F_V spectra in cyanobacteria, changes markedly with the excitation wavelength. As already mentioned, recording of emission spectra under F_M conditions, at room/physiologically relevant temperatures, is relatively straightforward. Observations of pronounced changes in the bandshape of the emission spectrum as a function of the excitation wavelength could then be used as a preliminary screening for indication of non-negligible contribution of pigment-protein complexes other than PSII to the cellular (or photosynthetic membrane) emission. If any independent knowledge is available concerning the spectral characteristics of the external antenna and/or of the PSI, which would help interpreting the F_M spectral excitation dependency, then appropriate pairs of excitation/detection wavelength can be chosen for classic fluorescence induction curve measurements.

To further highlight the importance of measurement conditions on the determination of the F_V/F_M ratio in cyanobacteria, in **Table 2** are reported the values of F'_0 , F_M and F_V/F_M which would be obtained monitoring these levels though collection by either interference or band-pass filters. Although the general trend is similar to what was reported for green algae in **Table 1**, the variations are much larger in the case of cyanobacteria where values exceeding 0.5 are obtained only for detection close to emission maximum (interferential at 685 nm) and avoiding preferential PBS excitation.

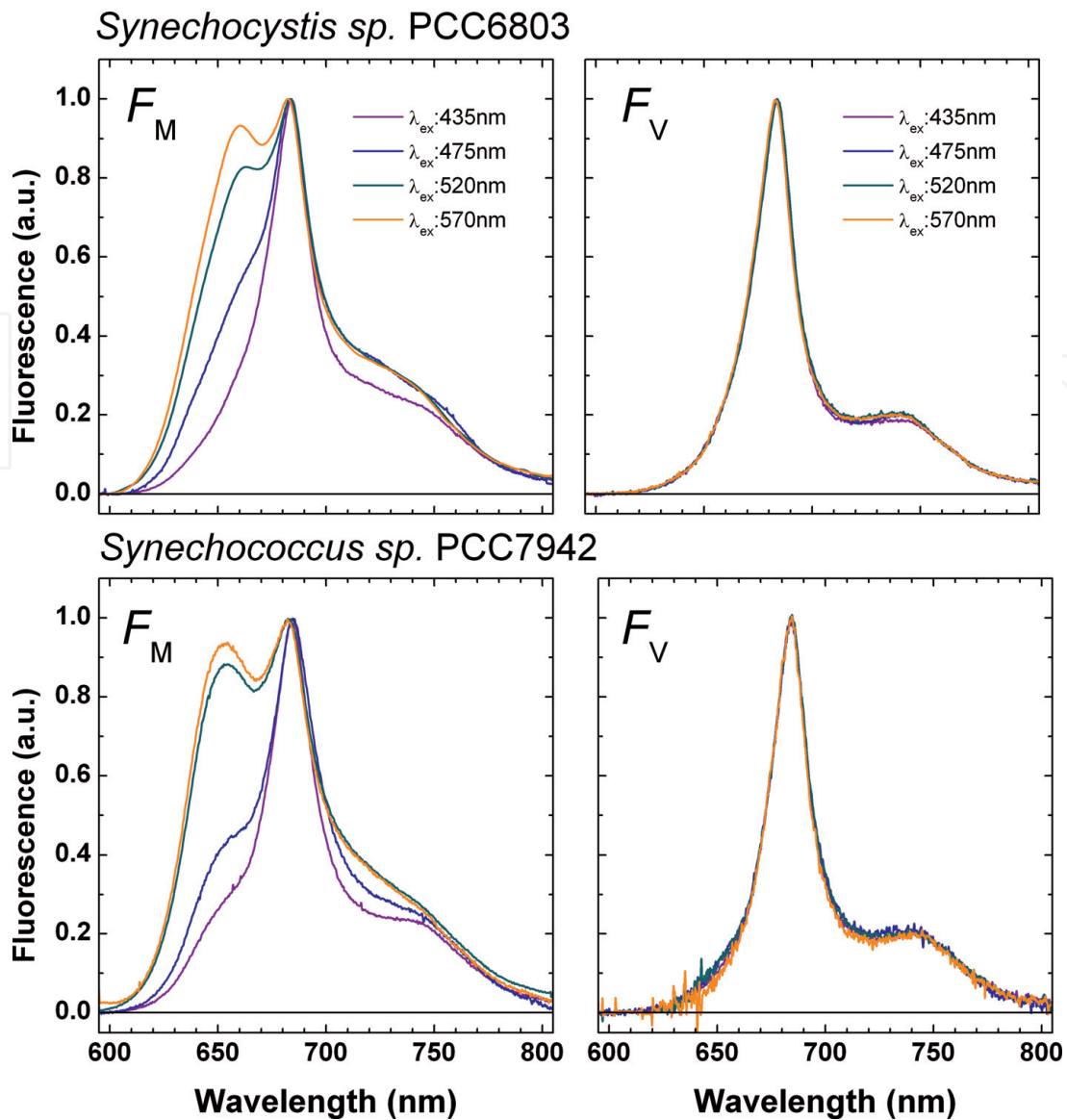


Figure 6. Comparison of the normalised F_M and calculated $F_V = F_M - F_0$ emission spectra, in *Synechocystis* sp. PCC6803 (top) and *Synechococcus* sp. PCC7942 (bottom), at room temperature, for excitation at 435 nm (violet), 475 nm (blue), 520 nm (green) and 570 nm (orange). Each spectrum is normalised to its maximum value.

2.3 Contribution of different chromophore-pigment super-complexes to photosynthetic membrane emission

The spectral dependencies of F_V/F_M could be accounted by a relatively simple formalism, based on considering a linear combination of contributions from i) PSII-antenna supercomplexes that give rise to variable fluorescence, F_V , and ii) other supercomplexes, in which the emission yield is independent of PSII redox state. The latter can be identified, in general terms, by the term F_{nV} that collectively accounts for emission of PSI and fractions of decoupled antenna, which are, as shown above, organism-dependent. Eq. (1) can be re-written, explicitly considering the excitation and emission dependency, as follows:

$$\begin{cases} F_0(\lambda_{em}, \lambda_{ex}) = \rho_{II}(\lambda) \cdot \sigma_{II}(\lambda) \cdot \phi_0 + \rho_{nV}(\lambda) \cdot \sigma_{nV}(\lambda) \cdot \phi_{nV} \\ F_M(\lambda_{em}, \lambda_{ex}) = \rho_{II}(\lambda) \cdot \sigma_{II}(\lambda) \cdot \phi_M + \rho_{nV}(\lambda) \cdot \sigma_{nV}(\lambda) \cdot \phi_{nV} \end{cases} \quad (5)$$

where $\rho_{II}(\lambda)$ and $\rho_{nV}(\lambda)$ are the absorption cross-sections of PSII and the pigments showing non-variable fluorescence, respectively; $\sigma_{II}(\lambda)$ and $\sigma_{nV}(\lambda)$ are the

<i>Synechocystis sp. PCC6803</i>								
Excitation	435 nm		475 nm		520 nm		570 nm	
Interferential (Centre, nm)	F'_0	F_V/F_M	F'_0	F_V/F_M	F'_0	F_V/F_M	F'_0	F_V/F_M
650	0.633	0.367	0.802	0.198	0.917	0.083	0.927	0.073
670	0.454	0.546	0.614	0.386	0.729	0.271	0.724	0.276
680	0.419	0.581	0.529	0.471	0.585	0.415	0.568	0.432
690	0.467	0.533	0.552	0.448	0.584	0.416	0.571	0.429
700	0.559	0.441	0.626	0.374	0.684	0.316	0.675	0.325
720	0.613	0.387	0.694	0.306	0.742	0.258	0.729	0.271
Bandpass (cut-on, nm)								
655	0.504	0.496	0.612	0.388	0.688	0.312	0.683	0.317
675	0.508	0.492	0.598	0.402	0.649	0.351	0.636	0.364
695	0.556	0.444	0.635	0.365	0.691	0.309	0.680	0.320
720	0.534	0.466	0.608	0.392	0.675	0.325	0.663	0.337
<i>Synechococcus sp. PCC7942</i>								
Interferential (Centre, nm)	F'_0	F_V/F_M	F'_0	F_V/F_M	F'_0	F_V/F_M	F'_0	F_V/F_M
650	0.750	0.250	0.866	0.134	0.955	0.045	0.972	0.028
670	0.487	0.513	0.678	0.322	0.775	0.225	0.803	0.197
680	0.413	0.587	0.598	0.402	0.629	0.371	0.663	0.337
690	0.446	0.554	0.631	0.369	0.630	0.370	0.666	0.334
700	0.530	0.470	0.710	0.290	0.729	0.271	0.766	0.234
720	0.547	0.453	0.722	0.278	0.774	0.226	0.806	0.194
Bandpass (cut-on, nm)								
655	0.491	0.509	0.677	0.323	0.731	0.269	0.761	0.239
675	0.479	0.521	0.663	0.337	0.691	0.309	0.720	0.280
695	0.516	0.484	0.697	0.303	0.728	0.272	0.756	0.244
720	0.498	0.502	0.677	0.323	0.708	0.292	0.730	0.270

Values of F'_0 and F_V/F_M determined from the F'_0 and F_M emission spectra of model cyanobacteria, after convolution with either ideal interferential filter (Gaussian, FWHM 10 nm) or long-pass filter (cut-on transitions 4 nm at the indicated 50% transmission). Values are normalised to $F_M = 1$ under each excitation/emission condition.

Table 2.

Estimated F'_0 and F_M detected through interferential and band-pass filters in cyanobacteria.

(area normalised) emission spectra of the same components; ϕ_{nV} , ϕ_0 and ϕ_M are the fluorescence yields of the non-variable component, PSII under open and closed centres, respectively, from which stems that

$$\begin{cases} F_V(\lambda_{em}, \lambda_{ex}) = F_M(\lambda_{em}, \lambda_{ex}) - F_0(\lambda_{em}, \lambda_{ex}) = \rho_{II}(\lambda) \cdot \sigma_{II}(\lambda) \cdot (\phi_M - \phi_0) \\ \frac{F_V}{F_M}(\lambda_{em}, \lambda_{ex}) = \frac{\rho_{II}(\lambda) \cdot \sigma_{II}(\lambda) \cdot (\phi_M - \phi_0)}{\rho_{II}(\lambda) \cdot \sigma_{II}(\lambda) \cdot \phi_M + \rho_{nV}(\lambda) \cdot \sigma_{nV}(\lambda) \cdot \phi_{nV}} \end{cases} \quad (6)$$

which satisfies the lack of excitation wavelength dependency of $F_V(\lambda_{em})$ and simply rationalise the differences in the value of F_V/F_M depending on the relative contribution of $F_{nV}(\lambda_{em}, \lambda_{ex})$. When this term tends to zero or being negligible with

respect to PSII emission at F_M , the expression is reduced to Eq. (2), and the estimation of $\Phi_{PC,PSII}^{Max}$ is relatively unbiased.

Recent reports from our laboratory have demonstrated that $F_{nV}(\lambda)$ at a given excitation wavelength could be extracted from the experimental spectra, simultaneously obtaining an estimation of $\Phi_{PC,PSII}^{Max}$ with reduced bias from spectral contributions other than PSII [26, 27]. In these studies, it was also shown that it was possible to separate spectrally the contributions of PSI and the uncoupled antenna, by considering the explicit contribution of these components to $F_{nV}(\lambda_{em}, \lambda_{ex})$:

$$F_{nV}(\lambda_{em}, \lambda_{ex}) = \rho_I(\lambda) \cdot \sigma_I(\lambda) \cdot \phi_I + \rho_{ul}(\lambda) \cdot \sigma_{ul}(\lambda) \cdot \phi_{ul} \quad (7)$$

where the absorption cross-section ($\rho_I(\lambda)$, $\rho_{ul}(\lambda)$), emission bandwidth ($\sigma_I(\lambda)$, $\sigma_{ul}(\lambda)$) and quantum yield (ϕ_I , ϕ_{ul}) of PSI and uncoupled antenna appear as independent terms. This expression is formally more correct because the fluorescence yield of the components not showing variable fluorescence is, in general, not the same. Eq. (7) can be straightforwardly used to replace the $F_{nV}(\lambda_{em}, \lambda_{ex})$ term in Eqs. (5) and (6).

In **Figure 7** are shown examples of the decomposition of the emission spectra of the green alga *C. sorokiniana* recorded under F'_0 and F_M conditions, by the independent contributions of PSI, PSII and uncoupled light harvesting antenna. Analogous results were obtained for *C. reinhardtii* [27]. The decomposition of the F'_0 and F_M spectra recorded in *Synechocystis* is instead shown in **Figure 8**, which, qualitatively, are representative also of the other model cyanobacterium considered, *Synechococcus*.

In accordance with qualitative data inspection of the spectra, in green algae, the emission spectra are largely dominated by PSII, and, even though the contribution of PSI is not negligible, the one of the uncoupled antenna, fundamentally, is so. The values of $\Phi_{PC,PSII}^{Max}$ derived from the spectral decomposition (0.715 for *C. sorokiniana* and 0.675 for *C. reinhardtii*) are only slightly higher (2–3%) than those obtained directly from the data, at their spectral maxima. This is moreover the case irrespectively of the excitation wavelength, as the same $\Phi_{PC,PSII}^{Max}$ was obtained for the decomposition at all excitation wavelengths [26, 27], and the F_V/F_M maximal values did not change greatly. On the other hand, the decomposition of the emission



Figure 7. Decomposition of the F'_0 and F_M emission spectra of *C. sorokiniana* in terms of independent contributions of PSI (wine lines), PSII (green lines) and uncoupled light-harvesting component, U-LHC, (blue lines). The black lines are the experimental spectra and the red lines are the results of the decomposition.

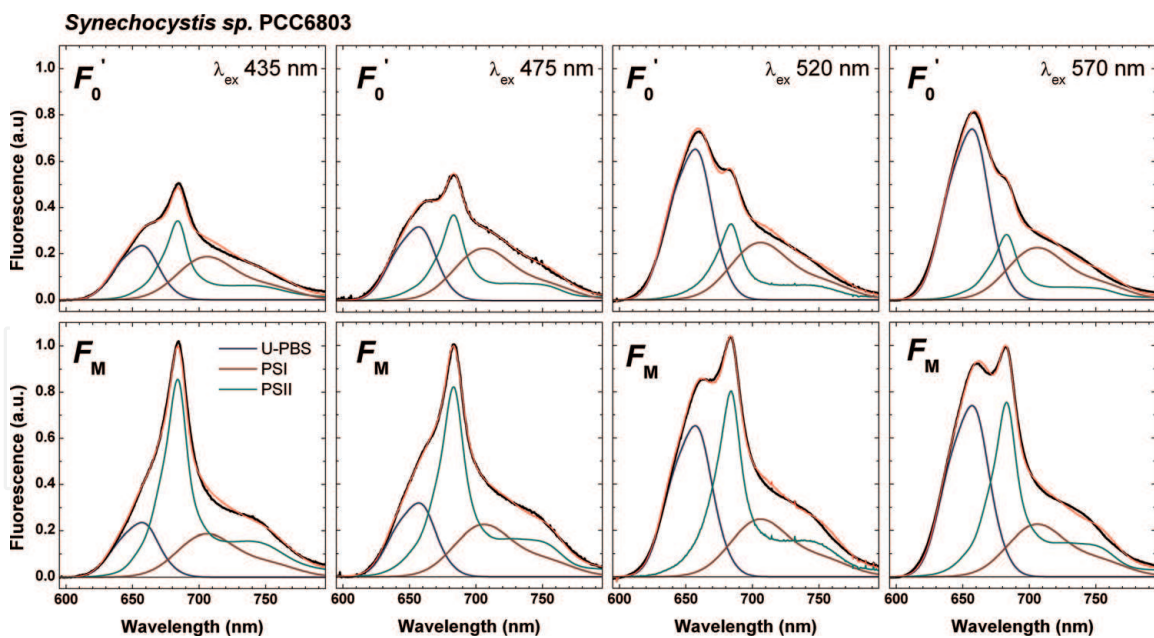


Figure 8.

Decomposition of the F_0' and F_M emission spectra in *Synechocystis* in terms of independent contributions of PSI (wine lines), PSII (green lines) and uncoupled phycobilisomes, U-PBS (blue lines). The black lines are the experimental spectra and the red lines are the results of the decomposition.

spectra of model cyanobacteria evidences not only a more significant contribution of PSI with respect to PSII, at all excitation wavelengths tested, but also an almost dominant contribution of the uncoupled PBS antenna upon its direct excitation. Thus, the values of $\Phi_{PC,PSII}^{Max}$ (0.625 for *Synechocystis* and 0.65 for *Synechococcus*) derived from decomposition, which was imposed to be excitation wavelength-independent, is in general much larger (35–40%) than those obtained directly from experimental data. The only conditions for which deviations are not extremely large are upon detection at maximal emission, 685 nm, and excitation at 435 nm. Under these conditions, the $\Phi_{PC,PSII}^{Max}$ is underestimated only by 5–7.5%. For detection above 700 nm, the underestimation of F_V/F_M is generally larger than 50% and can be up to 75%.

A relatively simple way to compensate for the contribution of the emission from pigment-protein complexes and supercomplexes that do not show variable fluorescence is that of applying a correction to the measured fluorescence levels. This however would in principle require independent evidences that the variable fluorescence spectrum is effectively independent of the excitation wavelength (as shown in **Figures 3** and **6**) and knowledge of the relative emission contribution of F_{nV} at a given pair of excitation/emission wavelengths. If the first condition is met, then F_V shall be considered to be unbiased, and a correction factor, $(\xi_{\lambda_{em},\lambda_{ex}})$, for F_M only would be necessary:

$$\left(\frac{F_V}{F_M}\right)_{\lambda_{em},\lambda_{ex}}^c = \frac{F_{V,\lambda_{em},\lambda_{ex}}}{F_{M,\lambda_{em},\lambda_{ex}}(1 - \xi_{\lambda_{em},\lambda_{ex}})} \quad (8)$$

A list of $\xi_{\lambda_{em}}$ values, for selected emission wavelengths, and for the excitation wavelengths discussed above, is reported in **Table 3**. Although these values are quite similar between the two green algae, and the two cyanobacteria, considered, it is nonetheless recommendable to use the correction parsimoniously, especially when this yields large increases with respect to the measured F_V/F_M and whenever possible to verify it under both the experimental conditions and the specific growth conditions of the organism. A recommended, empirical, check is represented by acquiring the F_V/F_M ratio at least at two pairs of excitation and emission

Excitation	<i>C. sorokiniana</i>				<i>C. reinhardtii</i>			
	435 nm	475 nm	520 nm	570 nm	435 nm	475 nm	520 nm	570 nm
Interferential (Centre, nm)								
650	0.02	0.03	0.05	0.03	0.02	0.03	0.02	0.03
670	0.02	0.02	0.03	0.02	0.02	0.03	0.02	0.03
680	0.02	0.01	0.02	0.02	0.01	0.02	0.02	0.02
690	0.02	0.02	0.03	0.02	0.02	0.03	0.03	0.04
700	0.06	0.04	0.07	0.06	0.04	0.07	0.06	0.08
720	0.09	0.07	0.11	0.09	0.04	0.07	0.06	0.08
Bandpass (cut-on, nm)								
655	0.04	0.03	0.06	0.04	0.03	0.04	0.03	0.05
675	0.05	0.04	0.06	0.05	0.03	0.04	0.04	0.05
695	0.07	0.05	0.09	0.07	0.04	0.06	0.05	0.06
720	0.06	0.05	0.08	0.06	0.03	0.04	0.04	0.05
Excitation	<i>Synechocystis sp. PCC6803</i>				<i>Synechococcus sp. PCC7942</i>			
	435 nm	475 nm	520 nm	570 nm	435 nm	475 nm	520 nm	570 nm
Interferential (Centre, nm)								
650	0.10	0.89	0.83	0.83	0.62	0.79	0.93	0.95
670	0.06	0.41	0.47	0.47	0.23	0.45	0.65	0.68
680	0.05	0.23	0.25	0.25	0.13	0.29	0.42	0.45
690	0.08	0.27	0.25	0.25	0.15	0.33	0.42	0.44
700	0.15	0.51	0.43	0.43	0.29	0.52	0.58	0.60
720	0.20	0.64	0.52	0.52	0.37	0.60	0.64	0.66
Bandpass (Cut-on, nm)								
655	0.11	0.46	0.42	0.42	0.24	0.46	0.57	0.59
675	0.12	0.43	0.37	0.37	0.22	0.43	0.50	0.51
695	0.16	0.58	0.44	0.44	0.28	0.51	0.55	0.56
720	0.15	0.57	0.41	0.41	0.24	0.46	0.48	0.49

Correction factors ($\xi_{\lambda_{em}, \lambda_{ex}}$) appearing in Eqs. (8), (10) and (11) derived for four excitation wavelengths, and for the expected emissions obtained for convolutions of either ideal interferential filters or long-pass filters (cut-on transitions 4 nm at the indicated 50% transmission).

Table 3.
 Correction factors compensating for non-variable fluorescence contributions at F_M .

wavelengths. If the corrected value yields, within errors, the same estimate of $\Phi_{PC,PSII}^{Max}$, then it is likely that the corrected value approaches the un-biased one.

3. Impact of the excitation/emission dependency on the NPQ estimations

Non-photochemical quenching of Chl fluorescence is one of the most intensively investigated regulative processes in oxygenic photosynthesis. As stated in the introduction, NPQ being an excited state quenching process, it is natural that fluorescence detection has been by far the most popular instrument to investigate it,

particularly *in vivo*. From the mechanistic point of view, NPQ results to be a very complex phenomenon, being controlled more or less synergically by an ensemble of effectors, whose specific action is species-dependent. Moreover, distinct NPQ processes that either develop or relax on different time scales have been reported, with the generally dominant ones being the rapidly forming/relaxing, energy-dependent quenching qE (e.g. [15–17]) and for prolonged illumination, the slowly/irreversible component, often associated with light-induced inhibition, qI component [15–17, 19]. The principal function of NPQ is that of regulating the rate of excitation delivery to the RC of PSII, by increasing the thermal dissipation in the antenna, under conditions in which the photosystem turnover can become limited by the availability of electron acceptors in the thylakoid electron transfer chain.

In land plants, and most green algae, the larger qE component of the NPQ process is dependent on the establishment of large pH gradients across the thylakoid membrane [15–17, 39]. However, whereas in land-plant, the presence of the PsbS subunit is crucial for a rapid and large NPQ establishment [15–19, 39, 40], in green algae, this is less fundamental, and the expression of specific light harvesting complexes (known as lhcs) has a more central role [39, 40]. Carotenoids, particularly those of the so-called xanthophyll cycle, also influence either the extent or the kinetics of formation/relaxation of NPQ [15–17, 19, 39, 40]. In both cases, the main effect is that of promoting the formation of quenching centres within the external antenna matrix of PSII, despite the site of quenching being still a matter of contention. As excited state equilibration within PSII is reached rapidly with respect to the excited state decay at F_M , the non-photochemical quencher could be considered, to a first approximation, to quench homogeneously the whole PSII-LHCII supercomplex.

The mechanisms of NPQ in cyanobacteria are understood in less detail. In these organisms, it has been shown that non-photochemical centres are also located in the external PBS antenna (reviewed in [17, 18, 40]) and that NPQ can occur even in mutants lacking the reaction centres [41, 42]. The induction of NPQ has a pronounced actinic light dependency, whose action spectrum closely matches the absorption of the orange carotenoid protein (OCP), which is a key factor in the sensing and possibly the induction of NPQ in this organism. In this scenario, it should then be considered that non-photochemical quenching could occur in the whole PSII-PBS supercomplex as well as in the uncoupled PBS fraction (as well as in both).

For the purposes of this chapter, a detailed discussion of the mechanisms of NPQ is not required, being the focus on the distortion of the measured Chl-based parameters, which for this process is through the “NPQ parameter” as defined in Eq. (4).

It is possible to estimate the extent of the bias originating from the emission of PSI and of the energetically uncoupled antenna fraction in a parameter, which shall reflect changes in the fluorescence yield of PSII, by simulating the cellular emission, starting from the decompositions obtained under measured F_M conditions, and by imposing selective non-quenching in PSII (or in PSII and/or the uncoupled antenna), thereby obtaining spectra under F'_M conditions, and successively comparing the NPQ which would be retrieved from experimental measurements with the *effective* one used in the simulations.

Using the same formalism adopted so far, when NPQ occurs in PSII only, the non-photochemically quenched emission at F'_M is described by:

$$\begin{cases} F'_M(\lambda_{em}, \lambda_{ex}) = \rho_{II}(\lambda) \cdot \sigma_{II}(\lambda_{ex}) \cdot \phi_{II,QN} + \rho_I(\lambda) \cdot \sigma_I(\lambda) \cdot \phi_I + \rho_{ul}(\lambda) \cdot \sigma_{ul}(\lambda) \cdot \phi_{ul} \\ \phi_{II,QN} = \frac{k_f}{\sum_i k_i + [Q_{NP}] \cdot K_{Q,NP}} \end{cases} \quad (9)$$

And when quenching in the uncoupled antenna fraction is necessary, ϕ_{ul} shall be substituted with $\phi_{ul,NQ}$, and, for simplicity we will consider, as a reasonable approximation, that $\phi_{ul} = \phi_M$. For simplicity, the case of cyanobacteria and green algae will be discussed separately.

3.1 Excitation and emission dependency of NPQ estimation in model green algae

The simulated fluorescence emission spectra in *C. sorokiniana* at F'_M conditions, compared with unquenched F_M , are presented in **Figure 9**. Values which would correspond to the NPQ parameters in the range of 1–4 for PSII emission were used in the simulations of the F'_M spectra. These values will be hereafter referred to as NPQ_{eff} . In the inset of the figures is shown the correlation between the NPQ_{eff} and the NPQ, which will be measured through interference filters centred at 660, 680, 700 and 720 nm, which cover most of the cellular emission bandwidth. For NPQ_{eff} levels below 2, the correspondence between the effective and detected NPQ is pretty good, particularly when the emission is monitored at 660 and 680 nm, as the deviation is between 5 and 10% of the imposed value. The correspondence is less satisfactorily when monitoring the emission at 700 and 720 nm, where deviations of

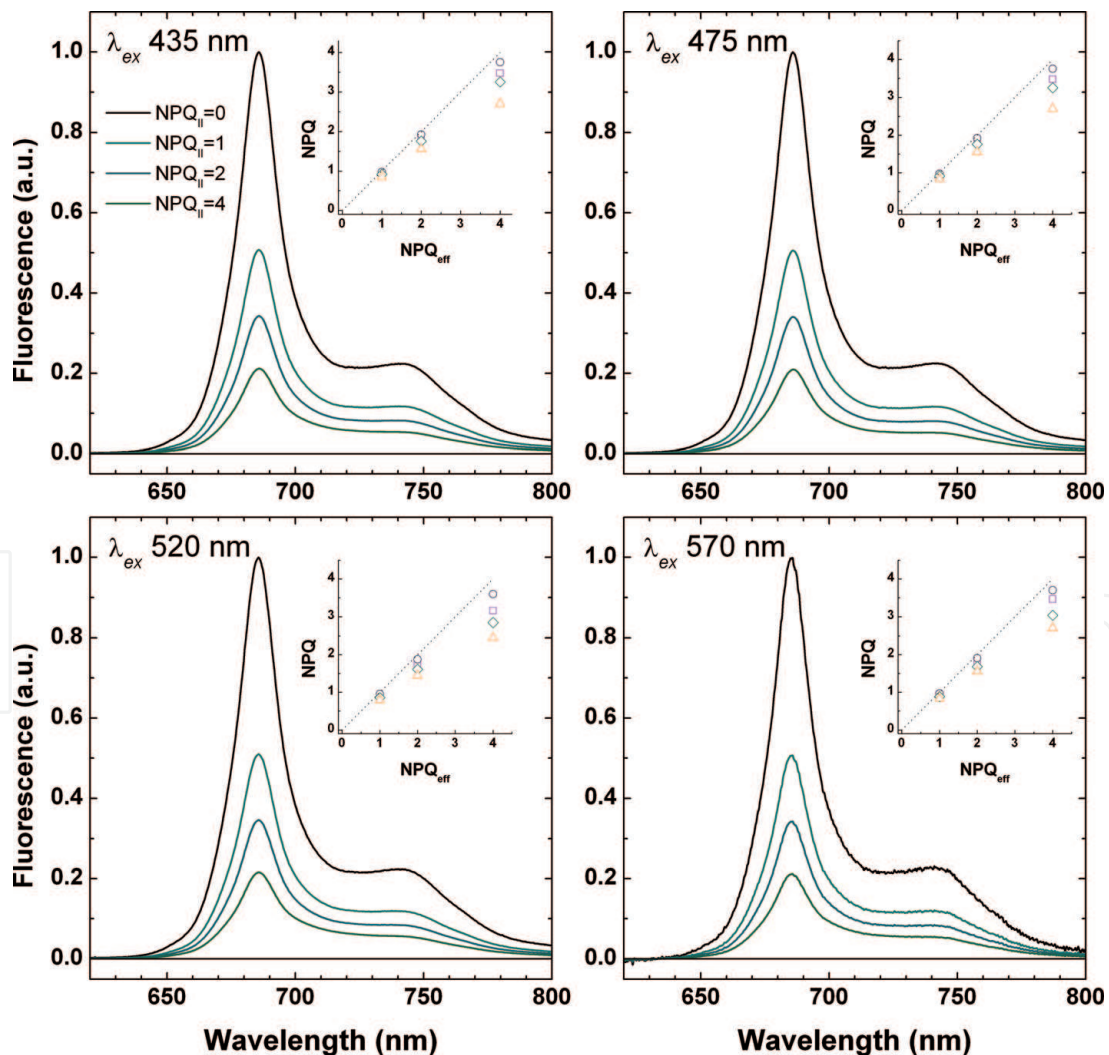


Figure 9. Simulations of F_M and F'_M spectra in the green alga *C. sorokiniana*. Spectra were simulated starting from the decomposition of **Figure 7** and by imposing quenching in PSII-LHCII only, corresponding to effective NPQ_{eff} values of 1, 2 and 4. The insets show the correlation between NPQ_{eff} and the detectable NPQ as it would be measured through interferential filters (FWHM 10 nm) centred at 660 (violet squares), 680 (blue circles), 700 (green diamond) and 720 nm (yellow triangles); the dashed lines correspond to un-biased estimations.

15–20% are estimated already for relatively limited quenching levels, particularly when exciting at 520 and 570 nm. In all cases, deviations are more significant for the largest NPQ_{eff} value tested of 4. This is a rather large value for green algae, which is rarely reported, but is worth testing in perspective. Moreover, an NPQ of 4 is almost equivalent to the maximal photochemical quenching at F_0 . When monitored at the maximal emission, NPQ is only about 10–15% underestimated, with the range depending on the excitation. Yet, for excitation in the yellow-green window and detection at 700 and 720 nm, the underestimation is in the 25–40% range, therefore significant.

The deviations between NPQ_{eff} and NPQ show a larger spectral dependence than the F_V/F_M ratio. This is due to the definition of the NPQ parameter, in which F'_M rather than F_M appears at the denominator. Since the contribution of any F_{nV} is expected to be the same under this condition, its relative weight would be larger on F'_M which is, by definition, smaller than F_M .

An alternative strategy to quantify non-photochemical quenching is via the non-photochemical quenching yield, (Φ_N , sometimes referred also to as q_N), which is defined as $\Phi_N = (F_M - F'_M)/F_M$. In analogy to F_V/F_M , within the large unit connectivity limit, Φ_N can be demonstrated to effectively represent a quenching yield, and therefore, its value falls between 0 and 1. Indeed, when estimating Φ_N , the deviation with respect to its expected value does not exceed 10%.

3.2 Excitation and emission dependency of NPQ estimation in model cyanobacteria

Using the same approach described above, the F'_M spectra were simulated also for the model cyanobacterium *Synechocystis sp.* PCC6803, considering the two scenarios in which NPQ occurs only in the PSII-PBS supercomplex (**Figure 10**) or in it as well as in the uncoupled PBS fraction (**Figure 11**). The same level of NPQ_{eff} (between 1 and 4) is applied to either PSII-PBS or both PSII-PBS and uncoupled PBS, and this value is compared to what is measured through interferential filters, at the same wavelengths already discussed, in the inset of the figures.

It is immediately apparent that, for the simulations of the F'_M spectra shown in **Figure 10**, the discrepancy between the putative measured and the imposed value is extremely large. Underestimations of less than 25% are predicted only for the smaller NPQ_{eff} value considered (1), when exciting preferentially Chl *a* (at 435 nm) and detecting at the maximal emission (680 nm). However, even under these detection conditions, the largest $NPQ_{\text{eff}} = 4$ simulated is predicted to be $\sim 40\%$ underestimated. Furthermore, the underestimations increase progressively with the increasing value of NPQ_{eff} under all measuring conditions simulated. At wavelengths in which PSI emission is significant (700 and 720 nm), NPQ underestimations are in the 60–80% range and always exceed 75%, being up to 95% when monitoring on the preferential PBS emission at 660 nm. As discussed for the case of green algae, the discrepancy between the effective and the predicted measured values is larger for NPQ than F_V/F_M , that were already significant, due to the largest weight of F_{nV} at F'_M rather than F_M .

The scenario is markedly different when considering quenching in both PSII-PBS and the uncoupled PBS. As shown in **Figure 11**, quenching is more obvious across a larger portion of the emission bandwidth, and this leads to a closer correspondence between NPQ_{eff} and the simulated detectable NPQ . In particular, the closest match between effective and measurable NPQ is in this scenario attained upon direct monitoring of the PBS emission at 660 nm, and upon their direct excitation at 520 and 570 nm, where deviations are always below 15% of the effective quenching value. For the estimations of NPQ when monitoring at the

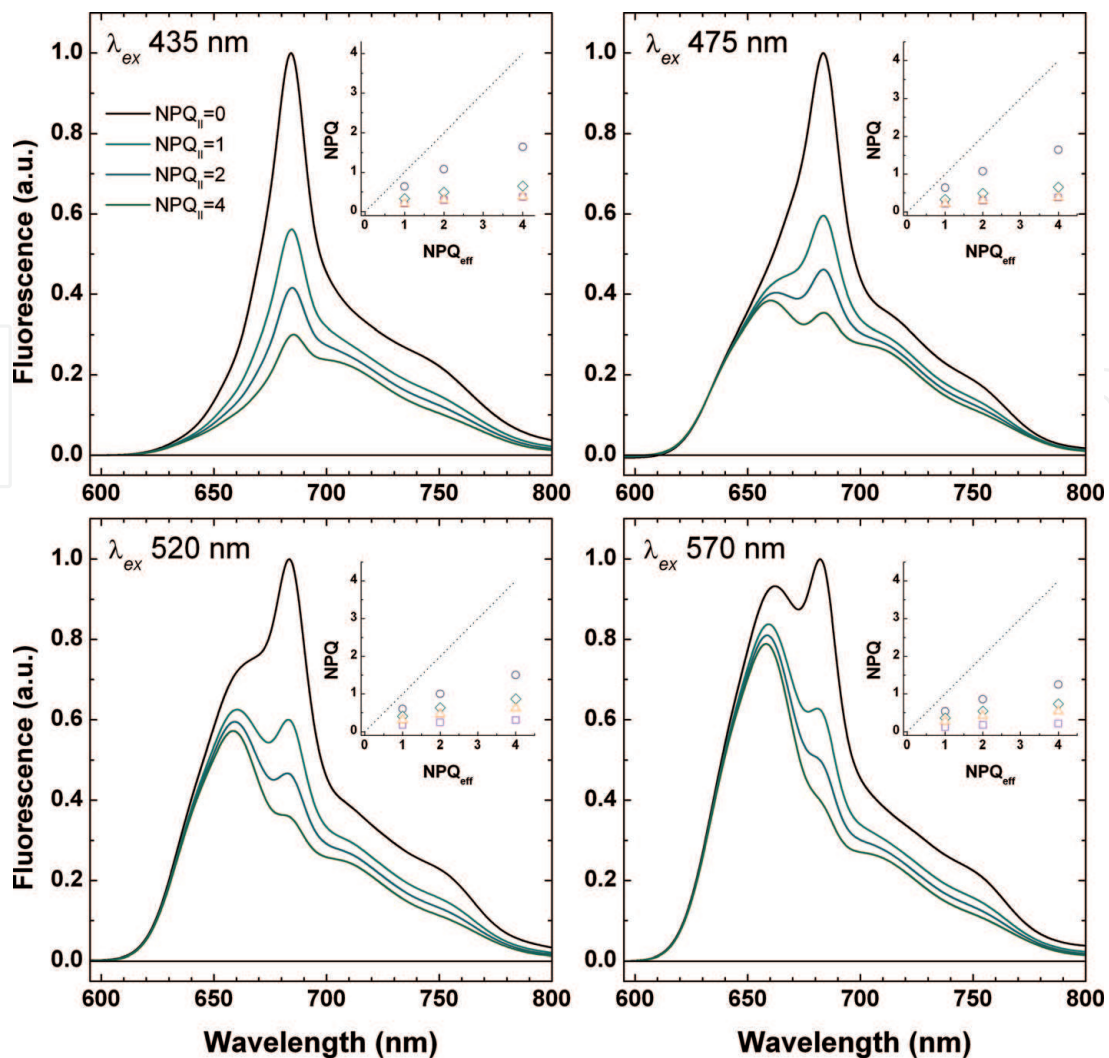


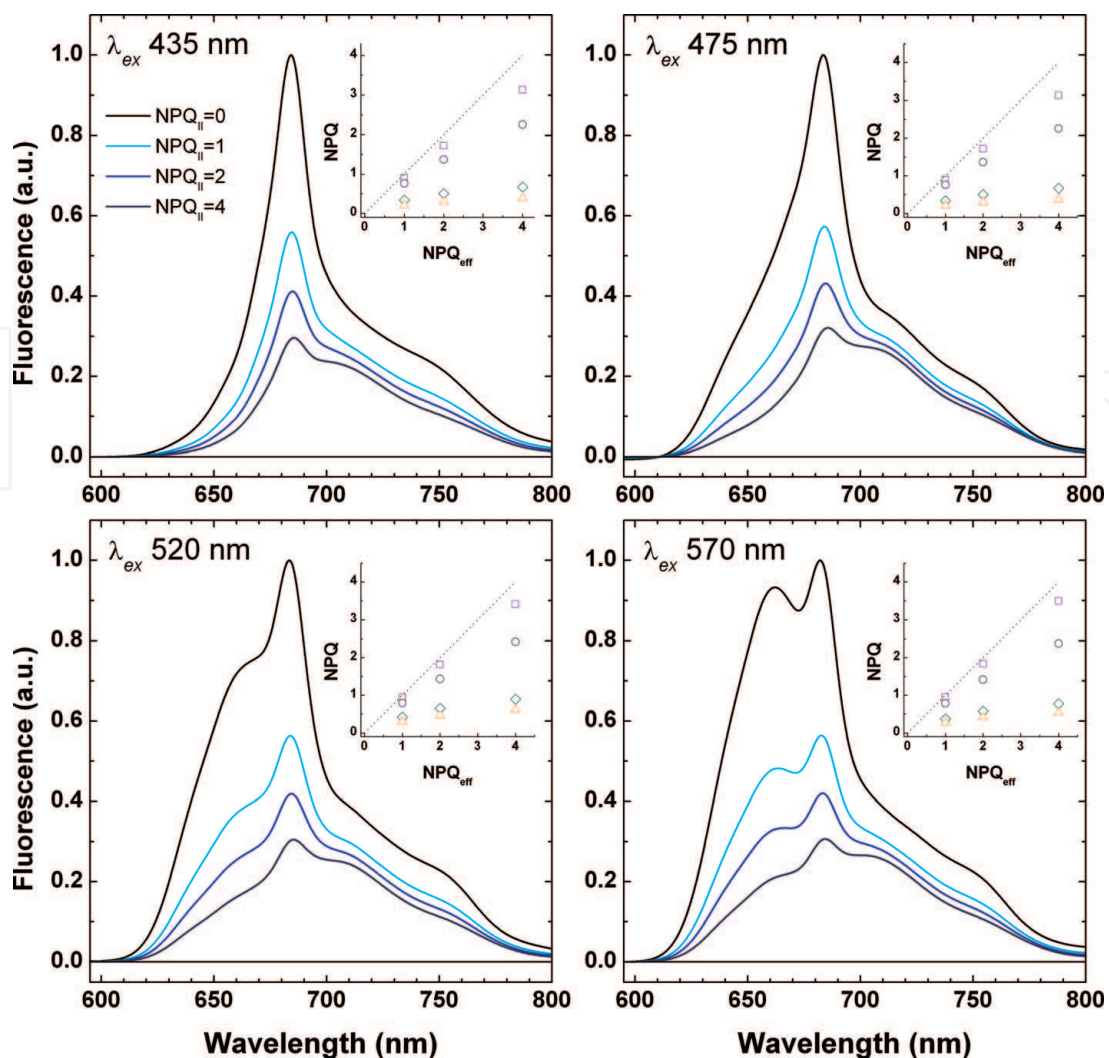
Figure 10. Simulations of F_M and F'_M spectra in the cyanobacterium *Synechocystis*. Spectra were simulated starting from the decomposition of **Figure 8** and by imposing quenching in PSII-PBS only, corresponding to effective NPQ_{eff} values of 1, 2 and 4. The insets show the correlation between NPQ_{eff} and the detectable NPQ as it would be measured through interferential filters (FWHM 10 nm) centred at 660 (violet squares), 680 (blue circles), 700 (green diamond) and 720 nm (yellow triangles); the dashed lines correspond to un-biased estimations.

maximal emission, a slightly closer correspondence is predicted when exciting in the blue (435 and 475 nm), but significantly larger values are predicted when exciting preferentially the PBS, despite remaining $\sim 40\%$ underestimated with respect to the effective ones. On the other hand, detection in the red tail (700 and 720 nm) leads to underestimation in the order of 60–80% irrespectively of the excitation wavelength. It is worth mentioning that differences in the spectra of **Figures 10** and **11** (and NPQ) might help in discriminating between the two different scenarios, or possible intermediate cases, experimentally.

The non-photochemical quenching yield, Φ_N , results less biased in both cases, however low-bias values (12%) for the scenario of **Figure 10** are predicted only for excitation at 435 nm and detection at 680 nm, whereas for the scenario of **Figure 11**, underestimations between 5 and 15% are predicted for detection at 660 and 680 nm, at all excitation wavelengths considered.

It is in principle possible to correct the measurement parameters, analogously to what is described in Eq. (8), provided the same caveats and even further recommendation of parsimony of use, so that the “corrected” NPQ parameter results:

$$NPQ_c = \frac{F_M - F'_M}{F'_M - \xi_{\lambda_{em}, \lambda_{ex}} \cdot F_M} \quad (10)$$


Figure 11.

Simulations of F_M and F'_M spectra in the cyanobacterium *Synechocystis*. Spectra were simulated starting from the decomposition of **Figure 8** and by imposing quenching in PSII-PBS and in the uncoupled PBS population. The same effective NPQ_{eff} values of 1, 2 and 4 were imposed in both. The insets show the correlation between NPQ_{eff} and the detectable NPQ as it would be measured through interferential filters (FWHM 10 nm) centred at 660 (violet squares), 680 (blue circles), 700 (green diamond) and 720 nm (yellow triangles); the dashed lines correspond to un-biased estimations.

and the photochemical quenching yield:

$$\Phi_{N,c} = \frac{F_M - F'_M}{F_M(1 - \xi_{\lambda_{em}, \lambda_{ex}})} \quad (11)$$

4. Conclusions

In this chapter, we discussed the influence of measurement settings on the determination of the two parameters, F_V/F_M and NPQ , which have a very widespread, routine, utilisation in photosynthesis research. A key caveat behind the physical interpretation is that the detected emission stems exclusively or almost exclusively from PSII. By comparing the excitation and emission dependency in two different classes of organisms, it is shown that, particularly in cyanobacteria, the emission from PSI and a fraction of uncoupled antenna, PBS in this case, can lead to large distortions, generally an underestimation, in the determination of F_V/F_M (as a proxy for $\Phi_{PC,PSII}^{Max}$) and even larger ones, of NPQ . Although the underestimation of

$\Phi_{PC,PSII}^{Max}$ in green algae is relatively limited, the one of NPQ can also be significant for large non-photochemical quenching.

Simple expressions for empirical correction of the measured F_M level are proposed, and the conditions for their validity and applicability are discussed.

Acknowledgements

This research was supported by: Fondazione Cariplo through the project “Cyanobacterial Platform Optimised for Bioproductions” (CYAO, ref. 2016-0667); sPATIALS3 project, financed by the European Regional Development Fund under the ROP of the Lombardy Region ERDF 2014-2020 - Axis I “Strengthen technological research, development and innovation” - Action 1.b.1.3 “Support for co-operative R&D activities to develop new sustainable technologies, products and services” - Call Hub; CNR project FOE-2019 DBA.AD003.139, BIO-ECO.

Conflict of interest

The authors declare no conflict of interest.

Author details

Stefano Santabarbara^{1*}, William Remelli¹, Anastasia A. Petrova^{1,3}
and Anna Paola Casazza²


¹ Photosynthesis Research Unit, National Research Council, Milano, Italy

² Istituto di Biologia e Biotecnologia Agraria, National Research Council, Milano, Italy

³ Belozersky Institute of Physico Chemical Biology, Moscow Lomonosov State University, Moscow, Russia

*Address all correspondence to: stefano.santabarbara@cnr.it

IntechOpen

© 2020 The Author(s). Licensee IntechOpen. Distributed under the terms of the Creative Commons Attribution - NonCommercial 4.0 License (<https://creativecommons.org/licenses/by-nc/4.0/>), which permits use, distribution and reproduction for non-commercial purposes, provided the original is properly cited. 

References

- [1] Papageorgiou GC, Govindjee, editors. Chlorophyll a fluorescence: A signature of photosynthesis. In: Advances in Photosynthesis and Respiration. Vol. 19. Dordrecht, The Netherlands: Springer; 2004
- [2] Joliot P, Joliot A. Etudes cinétique de la réaction photochimique libérant l'oxygène au cours de la photosynthèse. Comptes rendus de l'Académie des Sciences. 1964;258:4622-4625
- [3] Butler WL. Energy distribution in the photochemical apparatus of photosynthesis. Annual Review of Plant Physiology. 1978;29:345-378
- [4] Duysens LNM. Transfer and trapping of excitation energy in photosystem II. Ciba Foundation Symposium. 1978;61:323-340
- [5] Baker NR. Chlorophyll fluorescence: A probe of photosynthesis *in vivo*. Annual Review of Plant Biology. 2008; 59:89-113
- [6] Searle GF, Tredwell CJ, Barber J, Porter G. Picosecond time-resolved fluorescence study of chlorophyll organisation and excitation energy distribution in chloroplasts from wild-type barley and a mutant lacking chlorophyll b. Biochimica et Biophysica Acta. 1979;545:496-507
- [7] Moya I, Hodges M, Briantais J-M, Hervo G. Evidence that the variable chlorophyll fluorescence in *Chlamydomonas reinhardtii* is not recombinant luminescence. Photosynthesis Research. 1986;10: 319-325
- [8] Holzwarth AR, Wendler J, Haehnel W. Time-resolved picosecond fluorescence spectra of the antenna chlorophylls in *Chlorella vulgaris*. Resolution of photosystem I fluorescence. Biochimica et Biophysica Acta. 1985;807:155-167
- [9] Hodges M, Moya I. Time-resolved chlorophyll fluorescence studies of photosynthetic membranes: Resolution and characterisation of four kinetic components. Biochimica et Biophysica Acta. 1986;849:193-202
- [10] Roelofs TA, Lee CH, Holzwarth AR. Global target analysis of picosecond chlorophyll fluorescence kinetics from pea chloroplasts. A new approach to the characterisation of the primary processes in photosystem II alpha- and beta-units. Biophysical Journal. 1992;61: 1147-1163
- [11] Schansker G, Tóth SZ, Holzwarth AR, Garab G. Chlorophyll a fluorescence: Beyond the limits of the Q_A model. Photosynthesis Research. 2014;120:43-58
- [12] Magyar M, Sipka G, Kovács L, Ughy B, Zhu Q, Han G, et al. Rate-limiting steps in the dark-to-light transition of photosystem II - revealed by chlorophyll-a fluorescence induction. Scientific Reports. 2018;8:2755-2763
- [13] Genty B, Briantais J-M, Baker NR. The relationship between the quantum yield of photosynthetic electron transport and quenching of chlorophyll fluorescence. Biochimica et Biophysica Acta. 1989;990:87-92
- [14] Genty B, Harbinson L, Briantais J-M, Baker NR. The relationship between non-photochemical quenching of chlorophyll fluorescence and the rate of photosystem 2 photochemistry in leaves. Photosynthesis Research. 1990;25:249-257
- [15] Horton P, Ruban AV, Walters RG. Regulation of light harvesting in green plants. Annual Review of Plant Physiology and Plant Molecular Biology. 1996;47:655-684
- [16] Ruban AV. Nonphotochemical chlorophyll fluorescence quenching:

- Mechanism and effectiveness in protecting plants from photodamage. *Plant Physiology*. 2016;**170**:1903-1916
- [17] Goss R, Lepetit B. Biodiversity of NPQ. *Journal of Plant Physiology*. 2015; **172**:13-32
- [18] Kirilovsky D, Kerfeld CA. The orange carotenoid protein in photoprotection of photosystem II in cyanobacteria. *Biochimica et Biophysica Acta*. 1817;**2012**:158-166
- [19] Caffarri S, Tibiletti T, Jennings RC, Santabarbara S. A comparison between plant photosystem I and photosystem II architecture and functioning. *Current Protein & Peptide Science*. 2014;**15**: 296-331
- [20] Neilson JA, Durnford DG. Structural and functional diversification of the light-harvesting complexes in photosynthetic eukaryotes. *Photosynthesis Research*. 2010;**106**: 57-57
- [21] Grossman AR, Bhaya D, Apt KE, Kehoe DM. Light-harvesting complexes in oxygenic photosynthesis: Diversity, control, and evolution. *Annual Review of Genetics*. 1995;**29**: 231-288
- [22] Croce R, van Amerongen H. Light-harvesting in photosystem I. *Photosynthesis Research*. 2013;**116**: 153-166
- [23] Gobets B, van Grondelle R. Energy transfer and trapping in photosystem I. *Biochimica et Biophysica Acta*. 2001; **1057**:80-99
- [24] Rizzo F, Zucchelli G, Jennings RC, Santabarbara S. Wavelength dependence of the fluorescence emission under conditions of open and closed photosystem II reaction centres in the green alga *Chlorella sorokiniana*. *Biochimica et Biophysica Acta*. 1837; **2014**:726-733
- [25] Byrdin M, Rimke I, Schlodder E, Stehlik D, Roelofs TA. Decay kinetics and quantum yields of fluorescence in photosystem I from *Synechococcus elongatus* with P700 in the reduced and oxidised state: Are the kinetics of excited state decay trap-limited or transfer-limited? *Biophysical Journal*. 2000;**79**:992-1007
- [26] Remelli W, Santabarbara S. Excitation and emission wavelength dependence of fluorescence spectra in whole cells of the cyanobacterium *Synechocystis sp.* PPC6803: Influence on the estimation of photosystem II maximal quantum efficiency. *Biochimica et Biophysica Acta*. 2018; **1859**:1207-1222
- [27] Santabarbara S, Villafiorita Monteleone F, Remelli W, Rizzo F, Menin B, Casazza AP. Comparative excitation-emission dependence of the F_V/F_M ratio in model green algae and cyanobacterial strains. *Physiologia Plantarum*. 2019;**166**:351-364
- [28] Kaňa R, Prásil O, Komárek O, Papageorgiou GC, Govindjee. Spectral characteristic of fluorescence induction in a model cyanobacterium, *Synechococcus sp.* (PCC 7942). *Biochimica et Biophysica Acta*. 2009; **1787**:1170-1178
- [29] Santabarbara S, Jennings RC. The size of the population of weakly coupled chlorophyll pigments involved in thylakoid photoinhibition determined by steady-state fluorescence spectroscopy. *Biochimica et Biophysica Acta*. 1709;**2005**:138-149
- [30] Mullineaux CW, Bittersmann E, Allen JF, Holzwarth AR. Picosecond time-resolved fluorescence emission spectra indicate decreased energy transfer from the phycobilisome to photosystem II in light-state 2 in the cyanobacterium *Synechococcus* 6301. *Biochimica et Biophysica Acta*. 1990; **1015**:231-242

- [31] Mullineaux CW, Holzwarth AR. Kinetics of excitation energy transfer in the cyanobacterial phycobilisome-photosystem II complex. *Biochimica et Biophysica Acta*. 1991;**1098**:68-78
- [32] Campbell D, Hurry V, Clarke AK, Gustafsson P, Öquist G. Chlorophyll fluorescence analysis of cyanobacterial photosynthesis and acclimation. *Microbiology and Molecular Biology Reviews*. 1998;**62**:667-683
- [33] Acuña AM, Snellenburg JJ, Gwizdala M, Kirilovsky D, van Grondelle R, van Stokkum IHM. Resolving the contribution of the uncoupled phycobilisomes to cyanobacterial pulse-amplitude modulated (PAM) fluorometry signals. *Photosynthesis Research*. 2016;**127**: 91-102
- [34] Acuña AM, Kaňa R, Gwizdala M, Snellenburg JJ, van Alphen P, van Oort B, et al. A method to decompose spectral changes in *Synechocystis* PCC 6803 during light-induced state transitions. *Photosynthesis Research*. 2016;**130**:237-249
- [35] Pfündel EE. Deriving room temperature excitation spectra for photosystem I and photosystem II fluorescence in intact leaves from the dependence of F_v/F_m on excitation wavelength. *Photosynthesis Research*. 2009;**100**:163-167
- [36] Pfündel EE, Klughammer C, Meister A, Cerovic ZG. Deriving fluorometer-specific values of relative PSI fluorescence intensity from quenching of F0 fluorescence in leaves of *Arabidopsis thaliana* and *Zea mays*. *Photosynthesis Research*. 2013;**114**: 189-206
- [37] Murata N. Uphill energy transfer from chlorophyll a to phycobilins in the blue-green algae *Anabaena variabilis* and *Anacystis nidulans*. In: Miyachi S, Katoh S, Fujita Y, Shibata K, editors. Special Issue of Plant and Cell Physiology, No. 3. Photosynthetic Organelles. 1977:9-13
- [38] Wang RT, Myers J. Reverse energy transfer from chlorophyll to phycobilin in *Anacystis nidulans*. In: Miyachi S, Katoh S, Fujita Y, Shibata K, editors. Special Issue of Plant and Cell Physiology, No. 3. Photosynthetic Organelles. 1977:3-7
- [39] Ruban VA. Evolution under the sun: Optimising light harvesting in photosynthesis. *Journal of Experimental Botany*. 2015;**66**:7-23
- [40] Niyogi KK, Truong TB. Evolution of flexible non-photochemical quenching mechanisms that regulate light harvesting in oxygenic photosynthesis. *Current Opinion in Plant Biology*. 2013; **16**:307-314
- [41] Rakhimberdieva MG, Kuzminov FI, Elanskaya IV, Karapetyan NV. *Synechocystis* sp. PCC 6803 mutant lacking both photosystems exhibits strong carotenoid-induced quenching of phycobilisome fluorescence. *FEBS Letters*. 2011;**585**:585-589
- [42] Kuzminov FI, Karapetyan NV, Rakhimberdieva MG, Elanskaya IV, Gorbunov MY, Fadeev VV. Investigation of OCP-triggered dissipation of excitation energy in PSI/PSII-less *Synechocystis* sp. PCC 6803 mutant using non-linear laser fluorimetry. *Biochimica et Biophysica Acta*. 2012;**1817**:1012-1021